

## ESR Spectra of Six-coordinate Cobalt(III) Tetraphenylporphyrin Cation Radicals Generated by Electrochemical Oxidation II.<sup>1)</sup> Axial Ligand and Solvent Effects

Kohji ICHIMORI, Hiroaki OHYA-NISHIGUCHI,\* Noboru HIROTA, and Kiyoko YAMAMOTO†

Department of Chemistry, Faculty of Science, Kyoto University, Sakyo-ku, Kyoto 606

†The Institute of Physical and Chemical Research, Wako, Saitama 351-01

(Received August 15, 1984)

The ESR spectra of the  $\pi$ -cation radical generated electrochemically from 5,10,15,20-tetraphenylporphyrinatocobalt(II),  $[\text{Co}^{\text{II}}(\text{tpp})]$ , have been observed in the presence of various anions and in solvents such as halogenated hydrocarbons, nitriles, ethers, ethanol, and organic acids. From the analyses of these spectra, the  $\pi$ -cation radical has been found to coordinate axially the anion or the solvent according to the order of its coordinating ability;  $\text{BF}_4^-$ ,  $\text{ClO}_4^-$ ,  $\text{PF}_6^-$ ,  $\text{NO}_3^-$  < nitriles < halogen anions < ethanol <  $\text{CF}_3\text{COO}^-$ ,  $\text{AcO}^-$ ,  $\text{SCN}^-$ ,  $\text{CN}^-$ . The singly-occupied molecular orbital has been assigned to be always  $a_{2u}\pi$  orbital regardless of the axial ligands. The spin densities on N and Co much increase due to the axial ligation. It has been further confirmed that the spin polarization mechanism mainly contributes to the appearance of the spin density on Co. These axial-ligand effects are quantitatively explained by a model calculation of the CNDO/2 MO method.

The redox behavior of metalloporphyrins has been widely investigated from biological and biochemical interests and it has been known that most of metalloporphyrins are converted into their  $\pi$ -cation radicals by the oxidation of their porphyrin rings as well as of their central metal ions.<sup>2)</sup> Some of natural porphyrins can be oxidized into their  $\pi$ -cation radicals under mild conditions,<sup>3)</sup> but such readily oxidizable porphyrins have been rarely found in synthetic ones so far. It has been found that by thermal and light activations 5,10,15,20-tetraphenylporphyrinatocobalt(III) chloride,  $[\text{Co}^{\text{III}}(\text{tpp})]\text{Cl}$ , in chlorinated hydrocarbons is converted partially and reversibly into a paramagnetic species, which was identified by ESR as the  $[\text{Co}^{\text{III}}(\text{tpp})]^{2+}$   $\pi$ -cation radical coordinating axially two chlorides.<sup>4)</sup> From the studies using electrochemical techniques,<sup>1,4b)</sup> it has been shown that this radical is also generated by the one-electron oxidation of  $[\text{Co}^{\text{III}}(\text{tpp})]\text{Cl}$  or the subsequent two-electron oxidation of  $[\text{Co}^{\text{II}}(\text{tpp})]$  in the same solvents with tetrabutylammonium chloride (TBACl) as a supporting electrolyte. On the other hand, when  $\text{TBABF}_4$  or  $\text{TBAClO}_4$  was used, a different paramagnetic species was produced. It was concluded from the ESR observation that the  $\pi$ -cation radical coordinates different anions which perturb its electronic state. These results motivate us to examine in detail the effects of the coexisting anions and solvents on the ESR spectra of the  $\pi$ -cation radical. The ESR spectroscopy is a powerful means for investigating the microscopic structures of the complexes in solutions. Therefore, we have examined the ESR spectra of the  $\pi$ -cation radical using various combinations of anions and solvents.

In this paper, we first describe which anions or solvents are coordinated by the  $\pi$ -cation radical under different conditions and then discuss their effects on the electronic state of the  $\pi$ -cation radical. Secondly, we have made a model calculation of closed-shell CNDO/2 MO method including the cobalt AO in order to fully understand the effect of axial ligation. The results of the calculation will be compared with the experimen-

tal results.

It has been known that the electronic states of natural porphyrins are perturbed by their axial ligands, which is related to the bioactivities of the enzymes containing metalloporphyrins.<sup>5)</sup> It is hoped that this results will be helpful for understanding their activities.

### Experimental

**Materials.**  $[\text{Co}^{\text{II}}(\text{tpp})]$  and  $[\text{Co}^{\text{III}}(\text{tpp})]\text{Cl}$  were prepared by method previously reported.<sup>6)</sup>  $[\text{Co}^{\text{III}}(\text{tpp})]\text{Br}$  and  $[\text{Co}^{\text{III}}(\text{tpp})]_2(\text{SO}_4)$  were prepared in a similar way using HBr and  $\text{H}_2\text{SO}_4$ , respectively, instead of HCl for  $[\text{Co}^{\text{III}}(\text{tpp})]\text{Cl}$  preparation.<sup>7)</sup> They were identified by elemental analyses and absorption spectra. Dichloromethane (DCM), acetonitrile (ACN), propionitrile (PCN), butyronitrile (BCN), and nitromethane were of spectroscopic grade and dried over Woelm 200 neutral alumina. Tetrahydrofuran (THF), 1,2-dimethoxyethane (DME), and dibromomethane (DBM) were distilled over  $\text{CaH}_2$  before use. Ethanol of spectroscopic grade was distilled over magnesium ethoxide immediately prior to use. Trifluoroacetic acid (TFA) and trifluoroacetic anhydride (TFAA) of special grade were used without further purification.  $\text{TBABF}_4$ ,  $\text{TBAClO}_4$ ,  $\text{TBACl}$ , and  $\text{TBABr}$  were commercially obtained.  $\text{TBABF}_4$  and  $\text{TBAClO}_4$  of polarographic grade were used without further purification.  $\text{TBABr}$  was recrystallized once from ethyl acetate–ether (3:1).  $\text{TBAPF}_6$ ,<sup>8a)</sup>  $\text{TBANO}_3$ ,<sup>8b)</sup> and  $\text{TBAF}^{8c)}$  were prepared according to the methods reported elsewhere.  $\text{TBAPF}_6$  and  $\text{TBANO}_3$  recrystallized twice from ethanol–water and benzene, respectively, were confirmed by elemental analyses.  $\text{TBAF}$  was stored in ether under nitrogen atmosphere. The salts were dried *in vacuo* at room temperature before use except for  $\text{TBACl}$  which was dried at 90°C. The preparations of dibenzo-18-crown-6 (DB18C6) complexes with potassium salts were carried out according to the methods given by Pedersen.<sup>9)</sup>

**Apparatus and Procedures.** The ESR spectra were taken with JEOL PE-3X or FE-3X spectrometer equipped with a temperature controller. The  $[\text{Co}^{\text{III}}(\text{tpp})]$   $\pi$ -cation radical was generated by electrochemical two-electron oxidation of  $[\text{Co}^{\text{II}}(\text{tpp})]$  otherwise noted, using various electrolytes and

solvents. The best temperature for the ESR measurement depended on the solvent. In most cases, the ESR spectra were measured at temperatures 10 to 20°C above the melting point of the solvent. The procedure for the ESR measurement combined with electrochemical technique and the method of *g*-value calibration were described previously.<sup>9</sup> Here we only mention the usage of tetrabutylammonium salts and DB18C6·KX complexes (X=CN<sup>-</sup>, SCN<sup>-</sup>, and AcO<sup>-</sup>). Some of the salts used here have been found to function both as the axial ligand source for the cation radical and as the supporting electrolytes. But those salts comprising such an anion as CN<sup>-</sup>, SCN<sup>-</sup>, or AcO<sup>-</sup> could not be used as the supporting electrolyte, since they are very hygroscopic and/or difficult to be purified. Thus on the occasion of introducing such anions into sample solution, DB18C6·KX was added to the solution together with TBAPF<sub>6</sub> which acts only as the supporting electrolyte.<sup>10</sup> This method of preparing the sample solution may be generally useful for studying anion effects in nonaqueous solvents in electrolysis. DB18C6 was confirmed to have no effect on the ESR spectra by itself.

### Results

The  $\pi$ -cation radical exists in solution as a free ion

or a complex with the coexisting anion or the solvent whose effect is reflected sensitively on the ESR spectrum. Table 1 shows the parameters of the  $\pi$ -cation radical. In the following the results are classified into several groups by the electrolyte and solvent, denoted as electrolyte/solvent. The electrolytes should also be recognized as the source of anions coordinated by the  $\pi$ -cation radical.

**TBAPF<sub>6</sub>, TBABF<sub>4</sub>, TBAClO<sub>4</sub>, TBANO<sub>3</sub>/DCM, DBM.** It was suggested in the previous paper<sup>9</sup> that the  $\pi$ -cation radical in the system of TBAClO<sub>4</sub>/DCM or TBABF<sub>4</sub>/DCM might be complexed with ClO<sub>4</sub><sup>-</sup> or BF<sub>4</sub><sup>-</sup>. This was deduced from the marked difference between the ESR spectra of these systems and that of TBACl/DCM system in which the  $\pi$ -cation radical was shown to coordinate the chloride. However, there was no direct evidence of BF<sub>4</sub><sup>-</sup> or ClO<sub>4</sub><sup>-</sup> ligation in the ESR spectra. We have tried to clarify whether or not the  $\pi$ -cation radical coordinates these anions by observing its ESR spectra in the *inert* solvent such as DCM or DBM in the presence of BF<sub>4</sub><sup>-</sup>, ClO<sub>4</sub><sup>-</sup>, PF<sub>6</sub><sup>-</sup>, and NO<sub>3</sub><sup>-</sup> (weak-ligand anions).

TABLE 1. ESR PARAMETERS OF Co<sup>III</sup> (tpp)  $\pi$ -CATION RADICAL

Solvent	Anion	Axial Ligand	<i>T</i>	<i>g</i> (±0.0002)	$\Delta H^a)$ mT	hfcc/mT		
			°C			Co	N	X <sup>b)</sup>
DCM	BF <sub>4</sub> <sup>-</sup>	c)	-70	2.0031	4.53	0.57	(0.18)	—
	ClO <sub>4</sub> <sup>-</sup>	c)	-70	2.0031	4.41	0.57	(0.18)	—
	PF <sub>6</sub> <sup>-</sup>	c)	-70	2.0031	4.52	0.57	(0.18)	—
	NO <sub>3</sub> <sup>-</sup>	c)	-70	2.0031	4.59	0.6	—	—
	SO <sub>4</sub> <sup>2-</sup>	c)	-60	2.0031	4.41	0.57	—	—
	F <sup>-</sup>	F <sup>-</sup>	-70	2.003	7.98	—	—	2.68
	Cl <sup>-</sup>	Cl <sup>-d)</sup>	-70	2.0029	8.0	1.03	0.28	0.22
	CN <sup>-</sup>	CN <sup>-</sup>	-55	2.0033	8.1	1.02	0.26	—
	SCN <sup>-</sup>	SCN <sup>-</sup>	-65	2.0028	9.1	1.20	(0.25)	—
	AcO <sup>-</sup>	AcO <sup>-</sup>	-74	2.0072	7.1	0.92	0.20	—
DBM	BF <sub>4</sub> <sup>-</sup>	c)	-48	2.0028	4.0	—	—	—
	ClO <sub>4</sub> <sup>-</sup>	c)	-45	2.0028	3.92	—	—	—
	PF <sub>6</sub> <sup>-</sup>	c)	-45	2.0029	3.9	—	—	—
	Cl <sup>-</sup>	Cl <sup>-</sup>	-48	2.0035	7.97	1.02	—	—
	Br <sup>-</sup>	Br <sup>-</sup>	-48	2.008	10.0	—	—	—
PCN	BF <sub>4</sub> <sup>-</sup>	PCN <sup>d)</sup>	-70	2.0034	4.46	0.60	0.19	—
	ClO <sub>4</sub> <sup>-</sup>	PCN <sup>d)</sup>	-70	2.0034	4.47	0.60	0.19	—
	PF <sub>6</sub> <sup>-</sup>	PCN	-65	2.0034	4.46	0.60	0.19	—
	Cl <sup>-</sup>	Cl <sup>-</sup>	-70	2.0035	8.55	1.10	0.26	0.22
	CN <sup>-</sup>	CN <sup>-</sup>	-60	2.0035	8.1	1.07	0.27	—
ACN	PF <sub>6</sub> <sup>-</sup>	ACN	-34	2.0038	4.76	—	—	—
BCN	PF <sub>6</sub> <sup>-</sup>	BCN	-70	2.0034	4.51	—	—	—
CH <sub>3</sub> NO <sub>2</sub>	BF <sub>4</sub> <sup>-</sup>	CH <sub>3</sub> NO <sub>2</sub>	-24	2.0037	4.83	—	—	—
	PF <sub>6</sub> <sup>-</sup>	CH <sub>3</sub> NO <sub>2</sub>	-30	2.0037	4.81	—	—	—
	ClO <sub>4</sub> <sup>-</sup>	CH <sub>3</sub> NO <sub>2</sub>	-26	2.0037	4.80	—	—	—
EtOH	BF <sub>4</sub> <sup>-</sup>	EtOH	-70	2.0042	4.36	—	—	—
	PF <sub>6</sub> <sup>-</sup>	EtOH	-70	2.0042	4.35	—	—	—
	Cl <sup>-</sup>	EtOH	-68	2.0041	4.33	—	—	—
	CN <sup>-</sup>	CN <sup>-</sup>	-65	2.0033	8.0	1.02	0.24	—
	SCN <sup>-</sup>	SCN <sup>-</sup>	-65	2.0030	9.0	1.2	—	—
DME+THF	BF <sub>4</sub> <sup>-</sup>	c)	-80	2.003	(3.55)	—	—	—
TFA+TFAA	—	CF <sub>3</sub> COO <sup>-</sup>	-30	2.0051	4.78	(0.65)	—	—
	BF <sub>4</sub> <sup>-</sup>	CF <sub>3</sub> COO <sup>-</sup>	-30	2.0052	4.81	(0.65)	—	—
	F <sup>-</sup>	CF <sub>3</sub> COO <sup>-</sup>	-30	2.0050	4.73	(0.65)	—	—
	Cl <sup>-</sup>	CF <sub>3</sub> COO <sup>-</sup>	-30	2.0051	4.70	(0.65)	—	—

a) Total peak-to-peak width including hfcc. b) Axial ligand. c) The  $\pi$ -cation radical was not ligated. d) Previous work.

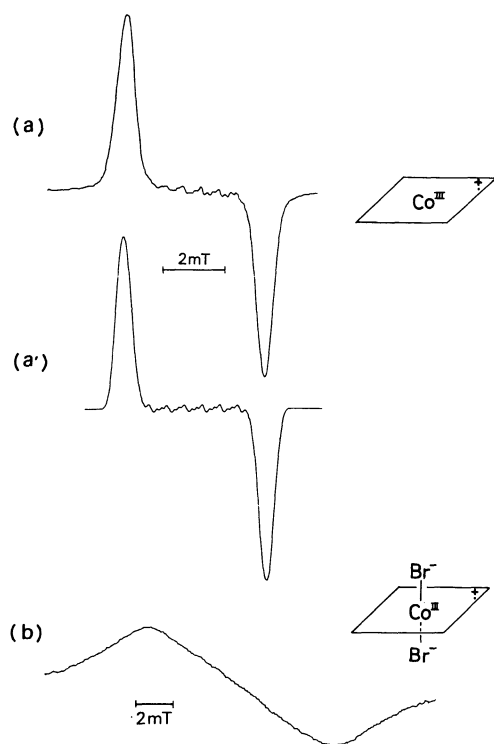


Fig. 1. The ESR spectra of  $[\text{Co}^{\text{III}}(\text{tpp})]$   $\pi$ -cation radical in the presence of weak-ligand anion and halogen anion: a)  $\text{TBABF}_4/\text{DCM}$  at  $-70^\circ\text{C}$ , a') The computer simulation of a), b)  $\text{TBABr}/\text{DBM}$  at  $-48^\circ\text{C}$ . The parallelograms in Figs. 1—3 indicate the porphyrin  $\pi$ -system.

The ESR spectra obtained in DCM did not depend on these anions, indicating that the  $\pi$ -cation radical did not coordinate these anions. A typical spectrum is shown in Fig. 1a. Partially resolved hyperfine structures (hfs) due to cobalt and nitrogen nuclei are seen in the spectrum. It is simulated with  $g=2.0031$ ,  $a_{\text{Co}}=0.57\text{ mT}$ ,  $a_{\text{N}}=0.18\text{ mT}$ , and linewidth of  $0.30\text{ mT}$ .

In DBM the anion dependence of the ESR spectra was not also observed. The hyperfine coupling constants (hfcc) could not be obtained from the ESR spectra because of line-broadening (Fig. 1b). The  $g$ -value and the total peak-to-peak width ( $\Delta H_{\text{pp}}$ ) were independent of the anions used (see Table 1). The possibility of the ligation of these anions was excluded, but there still remained the possibility of solvent ligation in these systems. The ligation of DBM is expected to cause a large  $g$ -value shift owing to the large spin-orbit interaction of bromine. Since the  $g$ -value was near that of free spin, it is concluded that the  $\pi$ -cation radical does not coordinate DBM. The  $g$ -value in DCM was almost equal to that in DBM and thus the same conclusion is derived for DCM, which is consistent with the inertness of DCM in ligation. The one-electron oxidation of  $[\text{Co}^{\text{III}}(\text{tpp})] (1/2)\text{SO}_4$  in  $\text{TBAPF}_6/\text{DCM}$  gave the same ESR spectrum as described above. Therefore, it is also concluded that the  $\pi$ -cation radical does not coordinate  $\text{SO}_4^{2-}$ .

*TBAF, TBACl, TBABr/DCM, DBM.* Halogen

anions are considered to have moderate coordinating ability and the  $\pi$ -cation radical is expected to coordinate these anions in the inert solvents.  $\text{TBACl}/\text{DCM}$  system has already been examined and Cl hfs was observed.<sup>11</sup> In  $\text{TBAF}/\text{DCM}$  system the ESR spectrum consisted of two components: a central sharp line ( $\Delta H_{\text{pp}}=1.5\text{ mT}$ ) and a broad line having two peaks on the both sides of the central line. The former was attributed to the  $\text{H}_2\text{tpp}$  radical generated by the loss of the cobalt ion, since there was no splitting due to the cobalt nuclei ( $I=7/2$ ). The latter showed an additional large splitting due to the fluorine nucleus ( $2.68\text{ mT}$ ), indicating that the  $\pi$ -cation radical coordinates the fluoride.

In  $\text{TBACl}/\text{DBM}$ , the  $\pi$ -cation radical coordinates the chloride as in  $\text{TBACl}/\text{DCM}$ . The ESR spectrum had a similar  $a_{\text{Co}}$  but was broader than that of in  $\text{TBACl}/\text{DCM}$ . In  $\text{TBABr}/\text{DBM}$  the presence of bromide gave a very broad ESR spectrum of the  $\pi$ -cation radical. The large  $g$ -value ( $2.008$ ) and  $\Delta H_{\text{pp}}$  ( $10\text{ mT}$ ) indicate the ligation of the bromide, but because of the broadness  $a_{\text{Co}}$  or  $a_{\text{Br}}$  could not be estimated (Fig. 1b). The one-electron oxidation of  $[\text{Co}^{\text{III}}(\text{tpp})]\text{Br}$  in  $\text{TBABr}/\text{DBM}$  gave the same spectrum.  $\text{TBAF}/\text{DBM}$  and  $\text{TBABr}/\text{DCM}$  systems gave no ESR spectra probably because the  $\pi$ -cation radical was unstable in these systems.  $\text{TBAI}$  was examined in both solvents, but no ESR spectra were observed.

#### *DB18C6·KCN, ·KSCN, ·KOAc+TBAPF<sub>6</sub>/DCM.*

Strong ligands such as  $\text{CN}^-$ ,  $\text{SCN}^-$ , and  $\text{AcO}^-$  were introduced in the form of DB18C6 potassium complexes mentioned in the previous section. These anions gave considerable changes to the ESR spectra and therefore the  $\pi$ -cation radical is considered to coordinate these anions. The cobalt hfcc's were comparable with that found for the radical complexed with chloride but varied somewhat depending on the anions.

Figure 2a gives the ESR spectrum of the  $\pi$ -cation radical in  $\text{DB18C6} \cdot \text{KCN} + \text{TBAPF}_6/\text{DCM}$  system, which shows well resolved hfs. The spectrum was simulated with one Co ( $a_{\text{Co}}=1.02\text{ mT}$ ), four N ( $a_{\text{N}}=0.26\text{ mT}$ ) and eight H ( $a_{\text{H}}=0.03\text{ mT}$ ) nuclei. The nitrogen hfs of the cyanide was not observed. This indicates that the cyanide is bound to the  $\pi$ -cation radical with the carbon, not the nitrogen. On the other hand, the spectrum in  $\text{DB18C6} \cdot \text{KSCN} + \text{TBAPF}_6/\text{DCM}$  system (Fig. 2b) could not be simulated with 1Co, 4N, and 8H. By taking the hfs due to the nitrogen nuclei of the thiocyanate into consideration, the spectrum was well simulated with 1Co ( $a_{\text{Co}}=1.20\text{ mT}$ ), 6N ( $a_{\text{N}}=0.25\text{ mT}$ ) and 8H ( $a_{\text{H}}=0.03\text{ mT}$ ), though there was an ambiguity of the  $a_{\text{N}}$  value. This result leads to the conclusion that the  $\pi$ -cation radical has N-bound thiocyanate in this system.

The acetate had a peculiar effect on the  $\pi$ -cation radical (Fig. 2c). Though the acetate does not contain a heavy atom, the  $g$ -value ( $2.0072$ ) was much larger than

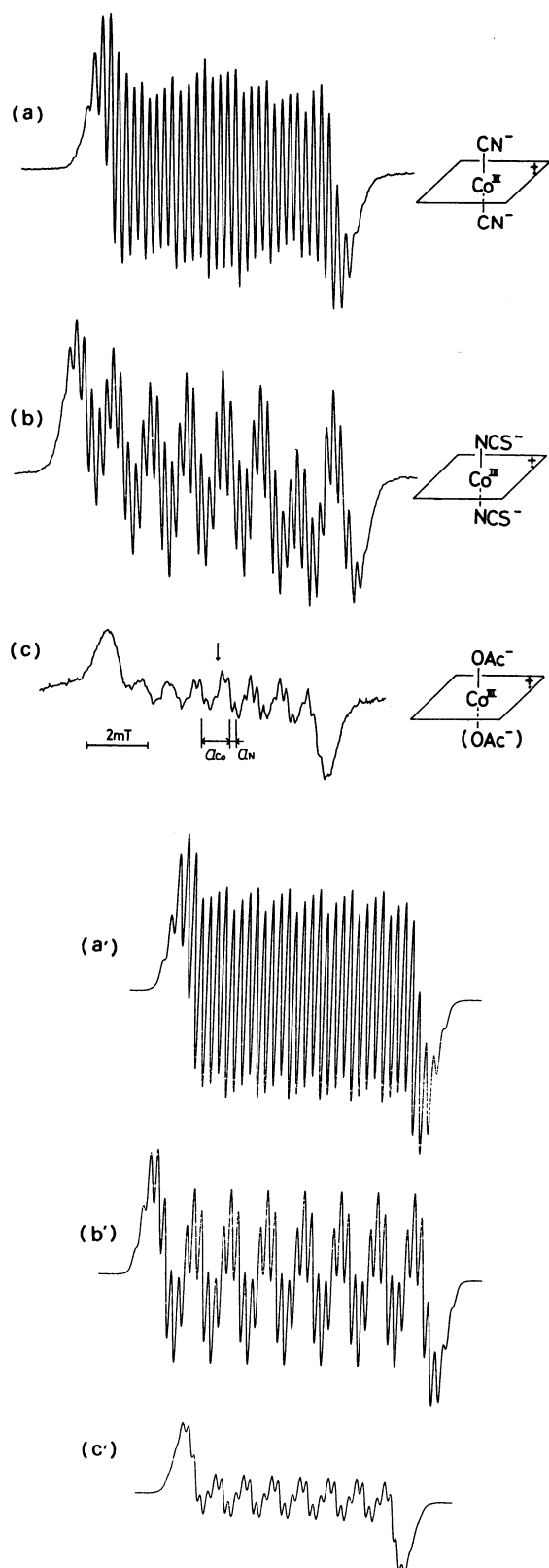


Fig. 2. The ESR spectra of  $[\text{Co}^{\text{III}}(\text{tpp})]$   $\pi$ -cation radical in the presence of strong ligands: a) DB18C6·KCN+TBAPF<sub>6</sub>/DCM at  $-55^\circ\text{C}$ , b) DB18C6·KSCN+TBAPF<sub>6</sub>/DCM at  $-65^\circ\text{C}$ , c) DB18C6·KOAc+TBAPF<sub>6</sub>/DCM at  $-74^\circ\text{C}$ , a'), b'), c') The computer simulations of a), b), and c), respectively. The linewidths of these spectra depend on  $\text{Co } m_I$ , but this effect was not considered in these simulations.

that of free spin. It has been said that the asymmetric axial ligation causes a large  $g$ -value of the  $\pi$ -cation radical (2.0056) in the case of  $[\text{Co}^{\text{III}}(\text{tpp})](\text{py})\text{Cl}$ .<sup>1)</sup> It is suggested that five-coordination or the up-and-down axial ligation by different ligands results in the displacement of the cobalt ion and the cobalt  $d$  orbital interacts with the singly-occupied  $a_{2u}$   $\pi$  orbital. In the case of the acetate, the  $\pi$ -cation radical is likely to be five coordinate or coordinate two oxygen atoms of the acetate, causing the large  $g$ -value shift mentioned above.

The ESR spectrum of DB18C6·KCl+TBAPF<sub>6</sub>/DCM system was identical with that of TBACl/DCM system. This result shows that the use of DB18C6 does not affect the ESR spectra.

#### *The Effect of Various Solvents in the Presence of Weak-ligand Anions.*

We also examined in detail the effects of other solvents, using the electrolytes comprised by  $\text{BF}_4^-$ ,  $\text{ClO}_4^-$ ,  $\text{PF}_6^-$ , and  $\text{NO}_3^-$ . As in the case of DCM or DBM, the ESR spectra did not depend on the coexisting anions. No hfs in the ESR spectra were observed except for the case of PCN. But the  $g$ -value and  $\Delta H_{pp}$  proved to be a good measure of the ligation state of the  $\pi$ -cation radical. As shown in Table 1, the  $g$ -values are different depending on the solvent, and are larger than 2.003, that is, the value in DCM or DBM. Thus it is concluded that the  $\pi$ -cation radical coordinates these solvents in the presence of weak-ligand anions.

#### *Solvent Effects in the Presence of Halogen Anions and Strong-ligating Anions.*

Since the halogen anions are nucleophiles and so the  $\pi$ -cation radical is subject to undergo reaction with them, the ESR spectra were observed only in a few cases. In TBACl/PCN reported previously,<sup>1)</sup> the ESR spectrum was almost the same as in TBACl/DCM, indicating that the chloride also is bound to the  $\pi$ -cation radical and the solvent had only a slight effect. On the other hand, the ESR spectra in EtOH did not change between the halogen anions and weak-ligand anions. This indicates that in EtOH the  $\pi$ -cation radical does not coordinate the halogen anions but EtOH. In both nitriles and EtOH, such anions as  $\text{CN}^-$ ,  $\text{SCN}^-$ ,  $\text{AcO}^-$  gave almost the same ESR spectra as in DCM, showing that the  $\pi$ -cation radical coordinates these anions.

In the mixed solvent of TFA and TFAA,  $\text{Co}^{\text{II}}(\text{tpp})$  was autoxidized into its  $\pi$ -cation radical. The ESR spectrum was easily observed with a large  $g$ -value (2.0050), which might be due to the effect of  $\text{CF}_3\text{COO}^-$  ligation as in the case of  $\text{AcO}^-$ . The ESR spectrum was not changed by the addition of the weak-ligand anions or the halogen anions. But the addition of  $\text{SCN}^-$  or  $\text{CN}^-$  gave the superimposed spectra of three species, the  $\Delta H_{pp}$  of which were 8 mT, 4 mT, and 1.5 mT. The corresponding species could be assigned as the  $\pi$ -cation radical binding  $\text{SCN}^-$  or  $\text{CN}^-$ , that binding  $\text{CF}_3\text{COO}^-$ , and that without the cobalt ion, respectively. Therefore, the coordinating ability of this solvent

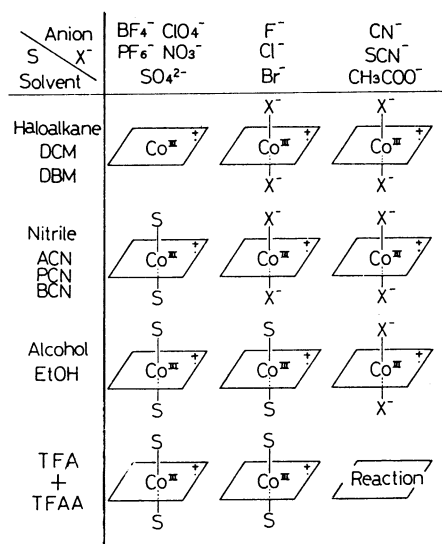


Fig. 3. A diagram for the structure of  $[\text{Co}^{\text{III}}(\text{tpp})]$   $\pi$ -cation radical in various solvents and in the presence of various anions.  $\text{X}^-$  and S denote coexisting anion and solvent, respectively.

competes with that of  $\text{SCN}^-$  or  $\text{CN}^-$ . Consequently, the order of coordinating ability to the  $\pi$ -cation radical is;  $\text{BF}_4^-$ ,  $\text{ClO}_4^-$ ,  $\text{PF}_6^-$ ,  $\text{NO}_3^-$ ,  $\text{SO}_4^{2-}$  < nitriles < halogen anions <  $\text{EtOH}$  <  $\text{CF}_3\text{COO}^-$ ,  $\text{AcO}^-$ ,  $\text{SCN}^-$ ,  $\text{CN}^-$ .

As described in the above sections, the states of axial ligation of the  $\pi$ -cation radical in various solvents and in the presence of various anions are clarified by the change of the ESR spectra. The results are summarized in Fig. 3. The  $\pi$ -cation radical coordinates the anion and solvent according to the order of coordinating ability, well-known as the spectrochemical series.

### Discussion

**The Axial-ligand Effect on the Electronic State of the  $\pi$ -Cation Radical.** As assigned first by the PPP-SCF MO calculation,<sup>12)</sup> the singly-occupied molecular orbitals (SOMO) of the two-electron oxidation products of cobalt porphyrins are  $a_{1u}$  or  $a_{2u}$   $\pi$  orbital in  $D_{4h}$  symmetry, not the 3d orbital of the cobalt ion. This has been confirmed by the fact that their  $g$ -values are quite isotropic and near the free-spin value. It has been considered that the  $a_{1u}$  and  $a_{2u}$  orbitals of metalloporphyrins are nearly degenerate.<sup>13)</sup> Indeed, in the case of  $\text{Co}(\text{oep})$  and  $\text{Co}(\text{etioporphyrin})$   $\pi$ -cation radicals, the order of the  $a_{1u}$  and  $a_{2u}$   $\pi$  orbitals changes depending on the counter ion: In the presence of weak-ligand anions or  $\text{F}^-$ , the  $a_{2u}$  orbital is the SOMO, while  $a_{1u}$  for  $\text{Br}^-$ .<sup>14)</sup> The nature of SOMO can be directly determined by the observation of nitrogen hfs, since the  $a_{2u}$  orbital has large spin densities on the nitrogen nuclei, but the  $a_{1u}$  has nodes on them. As shown in Table 1, the nitrogen hfs of the order of 0.2 mT was observed regardless of the nature of the ligands. Thus it is concluded that the SOMO is always the  $a_{2u}$  orbital different from the oep or etioporphyrin cases. It is note-

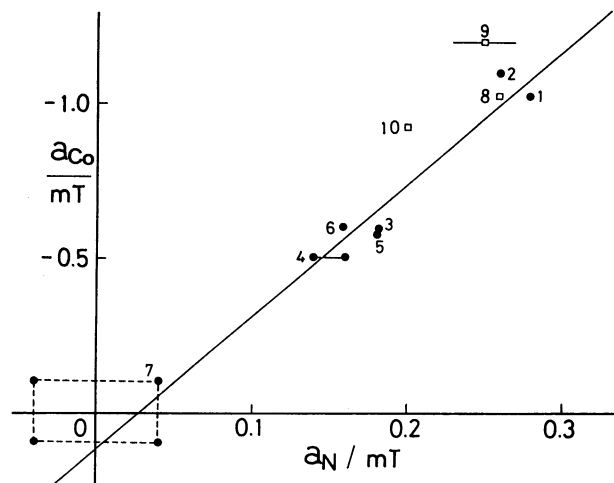


Fig. 4. A correlation between  $a_{\text{Co}}$  and  $a_{\text{N}}$  of some  $\text{Co}(\text{III})$  porphyrin  $\pi$ -cation radicals; 1:  $[\text{Co}^{\text{III}}(\text{tpp})]\text{Cl}_2$  (in DCM), 2:  $[\text{Co}^{\text{III}}(\text{tpp})]\text{Cl}_2$  (in PCN), 3:  $[\text{Co}^{\text{III}}(\text{tpp})](\text{BF}_4)_2$  (in DCM), 4:  $[\text{Co}^{\text{III}}(\text{tpp})](\text{ClO}_4)_2$  (in DCM), 5:  $[\text{Co}^{\text{III}}(\text{tpp})](\text{ClO}_4)_2$  (in BCN), 6:  $[\text{Co}^{\text{III}}(\text{pr})_4\text{p}](\text{ClO}_4)_2$  (in BCN), 7:  $[\text{Co}^{\text{III}}(\text{oep})](\text{ClO}_4)_2$  (in DCM), 8:  $[\text{Co}^{\text{III}}(\text{tpp})](\text{CN})_2$  (in DCM), 9:  $[\text{Co}^{\text{III}}(\text{tpp})](\text{SCN})_2$  (in DCM), 10:  $[\text{Co}^{\text{III}}(\text{tpp})](\text{OAc})_2$  (in DCM). This figure is composed by the addition of strong ligand cases ( $\square$ : 8–10) to Fig. 4. in Ref. 1.

worthy that the nitrogen hfs is increased by axial ligation.

The ESR spectra of the  $\pi$ -cation radical exhibit the  $^{59}\text{Co}$  hfs ( $a_{\text{Co}} = 0.5\text{--}1.2\text{ mT}$ ), which indicates that there is a small spin density on the central cobalt ion (at most 0.9%). In  $D_{4h}$  symmetry  $a_{2u}$  orbital and cobalt s and d orbital cannot overlap with each other. Thus it is necessary to consider a mechanism to interpret the  $^{59}\text{Co}$  hfs.

It has been proposed that there is a linear relationship between  $a_{\text{N}}$  and  $\rho_{\text{N}}^{\pi}$ , represented by

$$a_{\text{N}} = Q_{\text{N-Co}}^{\text{Co}} \times \rho_{\text{N}}^{\pi} + \alpha \quad (1)$$

where  $Q_{\text{N-Co}}^{\text{Co}}$  is a proportionality constant and  $\rho_{\text{N}}^{\pi}$  is the  $\pi$ -electron spin density on the nitrogen nuclei. The first term represents the contribution from the spin polarization of the  $\sigma$ -electrons in the Co–N bonds by the  $\pi$ -electron spin density on the nitrogen nuclei. The second term means the contribution from the direct overlap between the  $a_{2u}$  orbital and the cobalt orbitals. Figure 4 shows a correlation between  $a_{\text{Co}}$  and  $a_{\text{N}}$  listed in Table 1, in addition to those reported previously.<sup>1)</sup> The validity of Eq. 1 is further confirmed by the present study. It is seen that  $\alpha$  in Eq. 1 is small. Therefore,  $a_{\text{Co}}$  is mainly produced by the spin polarization mechanism. But when the  $\pi$ -cation coordinates  $\text{SCN}^-$  or  $\text{AcO}^-$ , there seems to be a slight deviation from the linear relationship, which is probably caused by the overlap between the p orbital of axial ligands and the  $a_{2u}$ .

**The CNDO/2 Calculations.** In order to explain the observed results, we have made CNDO/2 MO calculations<sup>19)</sup> extended to treat metal ions. The parameters used in these calculations are listed in Table 2.

TABLE 2. THE CNDO/2 PARAMETERS

Atom		H	C	N	F	Cl	Co
$\zeta^a$	s	1.2	1.6083	1.9237	2.5638	2.033	1.423
	p		1.5679	1.9170	2.5500	2.033	1.423
	d						2.830
$(I_p + A_p)/2(\text{eV})^b$	Ref.	14	15	15	15	15	16
	s	7.176	14.051	19.316	32.272	21.591	4.176
	p		5.572	7.275	11.180	8.708	1.160
$-\beta_A^\circ(\text{eV})^c$	d						5.839
	s	9	21	25	39	22.33	17.1
	p		21	25	39	22.33	4.76
	d						28.0

a) Basis set exponentials. b) The average potentials between ionization potential ( $I_p$ ) and electron affinity ( $A_p$ ) from Ref. 17. c) Bonding parameters from Refs. 15 and 18, Case III.

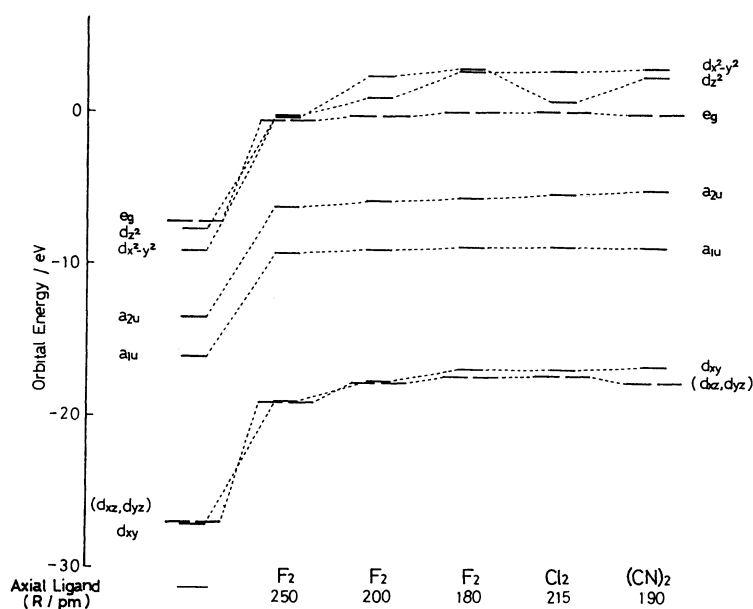


Fig. 5. Molecular orbital energy levels for  $[\text{Co}^{\text{III}}(\text{tmp})]\text{X}_2$  ( $\text{X}=\text{F}, \text{Cl}, \text{CN}$ ).  $R$  denotes Co-X distance. The d orbitals in this figure denote those orbitals whose electron densities are distributed mainly on the Co 3d orbital (at least 60%). The other orbitals can be characterized as the tmp  $\pi$  orbital.

The geometry of the porphyrin skeleton was obtained from a crystallographic study of  $[\text{Co}^{\text{II}}(\text{tpp})]$   $S_4$  symmetry.<sup>20</sup> The phenyl groups were replaced with methyl groups for simplifying the calculations. The geometries of the methyl groups were estimated from covalent radii and angles as well as those of hydrogen atoms attached to the pyrrole rings. From the ESR investigations of the  $\pi$ -cation radical of 5,10,15,20-tetraphenylporphyrinatozinc(II),  $\text{Zn}^{\text{II}}(\text{tmp})$ , the property of its SOMO has been known to be almost the same as that of  $\text{Zn}^{\text{II}}(\text{tpp})$   $\pi$ -cation radical.<sup>13,21</sup> Then the tmp skeleton was used instead of the tpp skeleton in our calculations. The axial ligands ( $\text{F}^-$ ,  $\text{Cl}^-$ , and  $\text{CN}^-$ ) were also placed on both sides of the tmp plane keeping the axial symmetry. The fluoride was placed at the distances of 250, 200, and 180 pm from the cobalt ion. From this one can estimate the effects of axial ligand field on the  $\pi$ -cation radical as a function of distance. The effects of the chloride and cyanide were also examined by taking their distances from the cobalt ion

as 215 and 190 pm, respectively, which were obtained from the crystal structure studies (116 pm for C-N distance).<sup>22,23</sup> The order of the ligand field strength is  $\text{F}^- < \text{Cl}^- < \text{CN}^-$ . The  $\pi$ -cation radical free from axial ligation ( $[\text{Co}^{\text{III}}(\text{tpp})]^{2+ \cdot}$ ) was also calculated for comparison.

The calculation was carried out under  $S_4$  symmetry. Figure 5 shows the calculated energy levels. Other results are listed in Table 3. Strictly speaking, the notations of  $a_{1u}$ ,  $a_{2u}$ , and  $e_g$  orbitals are only appropriate in  $D_{4h}$  symmetry, but they are also used here conventionally. The SOMO is always the  $a_{2u}$   $\pi$  orbital in agreement with the ESR observations mentioned above. The energy difference between the  $a_N$  and  $a_{Co}$  orbitals is quite large in each case compared with the energy shift due to the axial ligand, which makes the  $a_{2u}$  always SOMO. Both orbitals grow slightly more unstable with the strength of the axial ligand field, the extent of which is slightly larger for  $a_{2u}$  than for  $a_{1u}$ . In  $\text{Co}(\text{oep})$  and  $\text{Co}(\text{etioporphyrin})$ , both  $\pi$  orbitals are energetically

TABLE 3. THE RESULTS OF CNDO/2 CALCULATIONS

$X^{\text{a)}}$ $R^{\text{b)}}$ /pm		—	F 250	F 200	F 180	Cl 215	CN 190
$\rho^{\text{c)}}$	Co	$3d_{x^2-y^2}$	0.83	0.28	0.25	0.12	0.08
		$3d_{z^2}$	0.01	0.01	0.02	0.03	0.03
		$4p_z$	5.43	0.01	0.16	0.41	0.44
	N	$2p_z$	4.97	7.24	8.41	8.88	9.92
	$C_{\text{meso}}$	$2p_z$	10.18	8.58	9.92	10.30	8.88
	$C_{\alpha}$	$2p_z$	0.84	0.31	0.33	0.30	0.22
	$X^{\text{a)}}$	$2s$	—	0.03	0.07	0.12	0.10
		$2p_z$	—	9.80	3.72	1.99	2.34
$a_N^{\text{d)}}$ /mT			0.138	0.201	0.233	0.247	0.267
Net Charge	Co		+0.915	+0.905	+0.909	+0.947	+0.529
	$X^{\text{a)}}$		—	-0.613	-0.584	-0.531	-0.341

a) Axial ligand. b) The distance between the Co and axial ligand. c) Electron spin density. d) See Text. e) For C. f) For N.

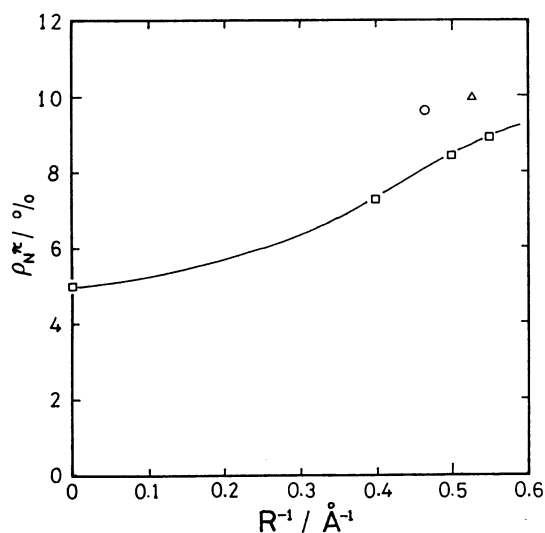


Fig. 6. A correlation between the spin density on the nitrogen nuclei ( $\rho_N^{\pi}$ ) and Co-X distance ( $R$ ) of  $[\text{Co}^{\text{III}}(\text{tmp})]\text{X}_2$   $\pi$ -cation radical (X: axial ligand);  $\square$ :  $[\text{Co}^{\text{III}}(\text{tmp})]\text{F}_2$ ,  $\circ$ :  $[\text{Co}^{\text{III}}(\text{tmp})]\text{Cl}_2$ ,  $\Delta$ :  $[\text{Co}^{\text{III}}(\text{tmp})](\text{CN})_2$ . The point at  $R^{-1}=0$  denotes  $[\text{Co}^{\text{III}}(\text{tmp})]^{2+}$   $\pi$ -cation radical free from axial ligation.

very close to each other and so small energy difference shift due to the change of axial ligand field causes the alternation of their SOMO. It is also noted that the energy of Co;  $3d_{z^2}$  orbital is strongly affected by the axial ligation, which is consistent with the prediction by the conventional crystal field theory for  $D_{4h}$  symmetry.

The spin density on the  $a_{2u}$  SOMO is mainly distributed on the nitrogen  $2p_z$  orbitals and the carbon  $2p_z$  orbitals at the meso positions as expected. Figure 6 shows the relation between the spin density on the nitrogen  $\pi$  orbitals ( $\rho_N^{\pi}$ ) and the distance between the cobalt ion and the axial ligands ( $R$ ). From the points for  $[\text{Co}^{\text{III}}(\text{tmp})]^{2+}$  and  $[\text{Co}^{\text{III}}(\text{tmp})]\text{F}_2$ , one can recognize that  $\rho_N^{\pi}$  becomes larger as the fluoride approaches the cobalt ion and reaches the value about twice as large as that of  $[\text{Co}^{\text{III}}(\text{tmp})]^{2+}$ . This is in good agreement with the experimentally observed trend that by the axial ligation  $a_N$  increased from 0.18 mT for the weak-ligand anions to 0.28 mT for  $\text{Cl}^-$ . The change from  $\text{F}^-$  to  $\text{Cl}^-$  and  $\text{CN}^-$  gives further small incre-

ment for  $\rho_N^{\pi}$ . Thus it is concluded that the ligand field strength plays the principal role in increasing  $\rho_N^{\pi}$ .

The  $a_N$ 's listed in Table 3 are calculated using the McConnell-type equation:  $a_N = Q_{\text{N}(\text{C}_2\text{H})}^{\text{N}} \rho_N^{\pi}$ , where  $Q_{\text{N}(\text{C}_2\text{H})}^{\text{N}}$  has the value of 2.78 mT, applicable to a nitrogen bonded to two carbon atoms and a proton.<sup>24)</sup> The calculated  $a_N$  for  $\text{Cl}^-$  or  $\text{CN}^-$  is in good agreement with the observed value. The  $a_N$  for a weak-ligand anion has the intermediate value between  $[\text{Co}^{\text{III}}(\text{tmp})]^{2+}$  and  $[\text{Co}^{\text{III}}(\text{tmp})]\text{F}_2$  ( $R=180$  pm) and so it is suggested that the weak-ligand anion exists in the vicinity of the cobalt ion, having an electrostatic effect on the  $a_{2u}$  SOMO.

The orbitals of the axial ligands directly overlap with  $a_{2u}$  SOMO, producing the hfs of the axial ligands. The calculated spin densities on the axial ligands have the value compatible with the observed hfs but the large ambiguity of the  $Q$ -value for F or Cl prevents us from making a quantitative discussion.

The cobalt  $4p_z$  orbital can mix with the SOMO. The lowering symmetry enables the cobalt  $3d_{x^2-y^2}$  and  $3d_{xy}$  to mix with the SOMO. In  $[\text{Co}^{\text{III}}(\text{tmp})]^{2+}$ , the spin density on the cobalt  $4p_z$  orbital is calculated to be large because of this mixing. However, even in the presence of weak-ligand anions, their electrostatic effects reduce this direct overlap between the cobalt orbitals and the SOMO. In fact, when the  $\pi$ -cation radical coordinates anions, these cobalt orbitals carry only at most 0.4% of spin density and cannot contribute so much to the  $^{59}\text{Co}$  hfs. Therefore, as mentioned in the previous part, the  $^{59}\text{Co}$  hfs is produced mainly by  $\rho_N^{\pi}$  through the spin polarization mechanism.

The authors are grateful to Dr. Hisayoshi Kobayashi of Kyoto Prefectural University for supplying them the program of CNDO MO calculation. They also express their thanks to the Data Processing Center of Kyoto University for the use of FACOM M-200 computer.

## References

- 1) Part 1: H. Ohya-Nishiguchi, M. Kohno, and K. Yamamoto, *Bull. Chem. Soc. Jpn.*, **54**, 1923 (1981).
- 2) D. G. Davis, "Electrochemistry of Porphyrins," in "The Porphyrins," ed by Dolphin, Academic Press Inc.,

New York (1978), Vol. 5, p. 127.

3) An interesting note with regard to horseradish peroxidase was reported: G. H. Loew and Z. S. Harman, *J. Am. Chem. Soc.*, **102**, 6173 (1980).

4) a) K. Yamamoto, J. Uzawa, and T. Chijimatsu, *Chem. Lett.*, **1979**, 89; b) K. Yamamoto, M. Kohno, and H. Ohya-Nishiguchi, *ibid.*, **1981**, 255.

5) W. D. Hewson and L. P. Hager, "Peroxidases, Catalases, and Chloroperoxidase," in "The Porphyrins," ed by Dolphin, Academic Press Inc., New York (1978), Vol. 7, p. 295.

6) K. Yamamoto and S. Tonomura. *Sci. Papers Inst. Phys. Chem. Res.*, **58**, 122 (1964).

7) K. Yamamoto. *Sci. Papers Inst. Phys. Chem. Res.*, **70**, 71 (1976).

8) a) E. C. Johnson. T. Niem. and D. Dolphin, *Can. J. Chem.*, **56**, 1381 (1978); b) N. L. Cox, C. A. Kraus, and R. M. Fuoss, *Trans. Faraday Soc.*, **31**, 749 (1935); c) E. J. Corey and A. Venkateswarlu, *J. Am. Chem. Soc.*, **94**, 6190 (1972).

9) C. J. Pedersen, *J. Am. Chem. Soc.*, **89**, 7017 (1967).

10) The DB18C6·KX complexes did not act well as supporting electrolyte.

11) The  $\Delta H_{pp}$  is given by  $\Delta H_{pp} = 7a_{Co} + \Delta H$ , where  $\Delta H$  is the linewidth,  $\Delta H_{pp}$  is used as a measure of  $a_{Co}$ , when  $a_{Co}$  is unresolved.

12) C. Weiss, H. Kobayashi, and M. Gouterman, *J. Mol. Spectrosc.*, **19**, 415 (1965).

13) J. Fajer and M. S. Davis, "Electron Spin Resonance of Porphyrin Cations and Anions," in "The Porphyrins," ed by Dolphin, Academic Press Inc., New York (1978), Vol. 4, p. 197.

14) D. Dolphin. A. Forman, D. C. Borg, J. Fajer. and R. H. Felton, *Proc. Nat. Acad. Sci. U. S. A.*, **68**, 614 (1971).

15) E. Clementi and D. L. Raimondi, *J. Chem. Phys.*, **38**, 2686 (1963).

16) M. Zerner and M. Gouterman, *Theor. Chim. Acta*, **4**, 44 (1966).

17) D. W. Clark, N. S. Hush, and J. R. Yandle, *J. Chem. Phys.*, **57**, 3503 (1972).

18) E. Kai and K. Nishimoto, *Int. J. Quantum. Chem.*, **18**, 403 (1980).

19) J. A. Pople and D. L. Beveridge, "Approximate Molecular Orbital Theory," McGraw-Hill, New York (1970), p. 57.

20) P. Madura and W. R. Scheidt, *Inorg. Chem.*, **15**, 3182 (1976).

21) J. Fajer, D. C. Borg, A. Forman, A. D. Adler, and V. Valedi. *J. Am. Chem. Soc.*, **96**, 1238 (1974).

22) T. Sakurai, K. Yamamoto, H. Naito, and N. Nakamoto, *Bull. Chem. Soc. Jpn.*, **49**, 3042 (1976).

23) A. Wolberg, *Acta Crystallogr., Sect. B*, **25**, 161 (1969).

24) J. R. Bolton, "Electron Spin Density," in "Radical Ions," ed by E. T. Kaiser and L. Kevan, John Wiley & Sons, New York. London. Sydney, (1968), p. 1.